

Enhanced gettering of gold at end-of-range defects in high energy ion implanted silicon

Satyabrata Mohapatra*

School of Basic and Applied Sciences, Guru Gobind Singh Indraprastha University, Dwarka, New Delhi 110078, India

*Corresponding author: Tel: (+91) 11 25302959; E-mail: smiuac@gmail.com

Received: 29 January 2017, Revised: 15 February 2017 and Accepted: 09 April 2017

DOI: 10.5185/amlett.2017.1648

www.vbripress.com/aml

Abstract

We report on the gettering behavior of Au at end-of-range (EOR) defects in float-zone grown Si(111), implanted with 1.5 MeV Au²⁺ ions at room temperature. The effects of implantation dose and annealing temperature on the thermal evolution of gettering behavior of EOR defects have been investigated using Rutherford backscattering spectrometry, while the microstructural evolution of Au implanted Si(111) has been studied using cross-sectional transmission electron microscopy combined with high resolution transmission electron microscopy. The gettering efficiency of EOR defects, comprising of dislocation loops, has been found to increase with increase in implantation dose up to 1.2×10^{15} ions cm⁻², beyond which it was found to saturate at about 5×10^{14} atoms cm⁻² for annealing at 850°C. We have observed that the gettering efficiency of the EOR defects for Au increased with increase in annealing temperature and reached 9×10^{14} atoms cm⁻² for annealing at 950°C. The observed enhanced gettering efficiency of EOR defects is very promising for gettering applications in Si devices. Copyright © 2017 VBRI Press.

Keywords: Ion implantation, defects, gettering, Au, Si.

Introduction

Ion implantation is extensively used in silicon technology due to its unique ability to precisely control the depth distribution and concentration of dopants. Post-implantation annealing is usually employed for damage recovery and electrical activation of dopants in Si. However, annealing results in transient enhanced diffusion (TED) of dopants which occurs due to the implantation damage [1-5]. During annealing the implantation damage in Si evolves into a supersaturation of excess Si interstitials, which precipitate on {311} planes as a single monolayer of hexagonal Si leading to the formation of rod-like defects running along <110> direction (known as {311} defects) [5-7]. For high dose amorphizing implants, extended defects such as end-of-range (EOR) dislocation loops are formed at the amorphous/crystalline interface during annealing due to the existence of a supersaturation of interstitials in the region [5-7]. These EOR dislocation loops affect the dopant distribution by capturing or releasing point defects during a subsequent thermal processing. The EOR defects lead to increased junction depth due to TED of dopants in Si [1-5], increased leakage current and hence result in deterioration of overall performance of Si devices [8-9]. Due to this a detailed understanding of the evolution of

extended defects at EOR and their interactions with point defects is necessary. The interaction kinetics between the EOR dislocation loops and the point defects has been shown to be diffusion limited and the evolution of EOR dislocation loops has been used to quantitatively measure the flux of point defects [10]. Diffusion of Au in Si is known to be mediated by either vacancies (Frank-Turnbull mechanism [11]) or Si interstitials (kick-out mechanism [12]). At temperatures $\geq 800^\circ\text{C}$, Au predominantly diffuses in Si via “kick-out” mechanism in which one interstitial Au atom (Au_i) knocks out a Si atom from its lattice site thereby becoming substitutional (Au_s). In the presence of sinks (trapping sites) for Si interstitials, an enhanced accumulation of immobile Au_s atoms takes place [13]. Hence, the trapping or detrapping of Au atoms at the EOR defects is controlled by the processes involving absorption or emission of Si interstitials respectively from these defects [13]. In other words, the resultant gettering Au concentration in EOR damage layer can be used as a probe to study the evolution of defects in EOR damage layer during thermal annealing. The aim of this study is to study the interactions between EOR defects and Si interstitials, through the gettering behaviour of EOR defects for Au atoms in Si(111).

In this study, we have investigated the effects of Au implantation dose and annealing temperature on the gettering efficiency of EOR defects for Si interstitials, using the gettering Au concentration in EOR damage layer as a probe.

Experimental

Float-zone (FZ) grown n-type Si(111) single crystal wafer ($\rho \sim 10 \Omega \cdot \text{cm}$) was used as substrates. FZ Si(111) substrates were implanted with 1.5 MeV Au²⁺ ions to doses varying from 4×10^{14} to 4×10^{15} ions cm⁻². The implantations with ion current density of about 100 nA cm⁻² were carried out at room temperature using 7° tilt angle to avoid ion channeling. Following implantation, one set of samples were annealed at 850°C for 1 h and were allowed to slowly cool down after annealing. One of the samples implanted with a dose of 2.2×10^{15} ions cm⁻² was isochronally annealed for 20 minutes in the temperature range of 550 - 950°C using 100°C steps. Each annealing step was followed by a rapid quenching in liquid N₂. Rutherford backscattering spectrometry (RBS) was used to analyze the samples after each annealing step to study the gettering behavior of defects and quantify the amount of Au gettered in different damage layers in Si(111). RBS analyses of the samples were carried out using 3.05 MeV He²⁺ ions with a Si surface barrier detector placed at a backscattering angle of 160°. All the ion implantations and RBS measurements were carried out using the 3 MV Pelletron accelerator facility at the Institute of Physics, Bhubaneswar. The microstructure of damage layers in Au implanted Si(111) before and after thermal annealing was studied using cross-sectional transmission electron microscopy (XTEM) and high resolution transmission electron microscopy (HRTEM). The samples for XTEM analysis were prepared using mechanical polishing followed by ion milling with 3 keV Ar ions. XTEM and HRTEM studies were carried out at 200 keV using JEOL 2010 UHR TEM facility at Institute of Physics, Bhubaneswar.

Results and discussion

Fig. 1 shows the RBS spectra showing redistribution of Au atoms in Si(111) implanted with 1.5 MeV Au²⁺ ions to four different doses varying from 4×10^{14} to 4×10^{15} ions cm⁻² upon 1 h annealing at 850°C. It can be clearly seen that while the Au profiles in all the as-implanted samples are Gaussian, annealing at 850°C for 1 h leads to significant redistribution of Au atoms. For a Au dose of 4×10^{14} ions cm⁻², annealing resulted in Au profile with a tailing towards the surface as can be seen from **Fig. 1(a)**. A small fraction of the implanted Au atoms out-diffused into the near-surface region, while an appreciable fraction remained trapped in the EOR damage layer. **Fig. 1(b)** shows the annealing induced redistribution of Au profile in Si(111) implanted with a dose of 1.2×10^{15} ions cm⁻². Annealing at 850°C led to significant redistribution of Au profile resulting in a bimodal depth distribution, with two distinct peaks emerging at the EOR damage layer and near-surface region. Increasing the Au dose to 2.2×10^{15} ions cm⁻² resulted in a marked enhancement in the intensity of Au peak in the near-surface region, with almost no change in the Au profile gettered at the EOR damage layer (**Fig. 1(c)**). Further increase in Au dose to 4×10^{15} ions cm⁻² led to significant out-diffusion of Au

atoms with appreciable enhancement in intensity and broadening of Au peak in the near-surface region, while the Au profile in the EOR damage layer remains mostly unchanged, as can be seen from **Fig. 1(d)**.

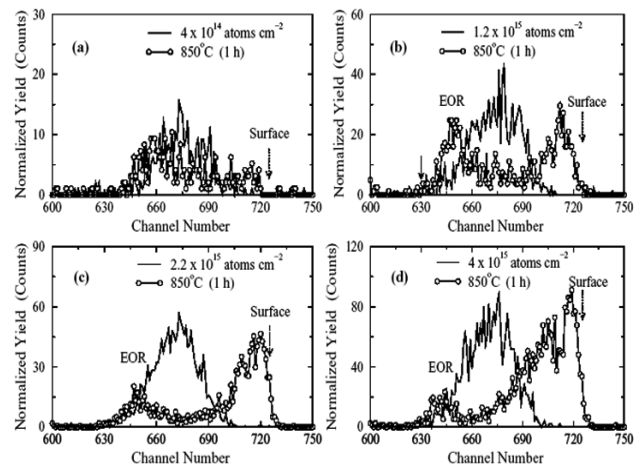


Fig. 1. RBS spectra showing Au profiles in Si(111) substrates implanted with 1.5 MeV Au²⁺ ions to different doses before and after annealing at 850°C for 1 h.

The Au dose dependence of the gettering efficiency of the EOR and near-surface damage layers is shown in **Fig. 2**. In the dose range of 4×10^{14} to 4×10^{15} ions cm⁻², the concentration of Au atoms gettered in the near-surface damage layer is found to increase almost linearly with an increase in Au dose. For the sample implanted with Au dose of 4×10^{15} ions cm⁻², the fraction of Au gettered in the near-surface damage layer reaches 87.5% (3.5×10^{15} ions cm⁻²) which is very high. Interestingly the Au dose dependence of the concentration of Au trapped in the EOR damage layer shows a saturation behavior. Initially the concentration of Au gettered in the EOR damage layer increased with increase in Au dose up to 1.2×10^{15} ions cm⁻², beyond which it was found to saturate at a value of about 5×10^{14} atoms cm⁻² even though Au dose is increased to 4×10^{15} ions cm⁻².

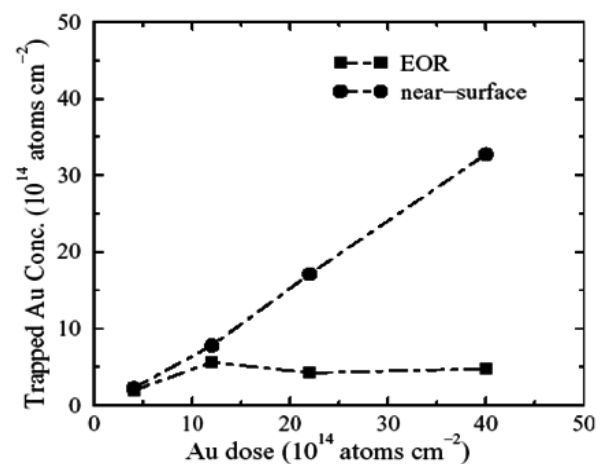


Fig. 2. Dependence of trapped Au concentration at EOR and near-surface damage layers on Au implantation dose for 1 h annealing at 850°C.

In order to understand the Au gettering behavior of EOR damage layer, RBS studies were carried out on another sample implanted with 1.5 MeV Au²⁺ ions to a dose of 2.2×10^{15} ions cm⁻² following isochronal annealing for 20 minutes in the temperature range of 550 - 950°C using 100°C steps, with each annealing step followed by a rapid quenching in liquid N₂. The RBS spectra showing the Au profiles in this sample following 20 minute sequential isochronal annealing steps at 550-950°C are shown in Fig. 3. The Au profile in the as-implanted sample (shown in Fig. 3 (a)) is found to be Gaussian. A small tailing towards the surface can be seen after annealing at 550°C (see Fig. 3 (b)). Annealing at 650°C led to a flat-topped Au profile reaching out to the surface. Further 20 minute annealing at 750°C, resulted in an enhanced out-diffusion of Au atoms to the near-surface region, with a small fraction trapped at the EOR damage layer (Fig. 3 (d)). Similar results showing annealing induced out-diffusion of implanted Au in Si (111) have been reported in an earlier study [14]. Subsequent 20 minute annealing at 850°C resulted in a marked back-diffusion of Au towards EOR damage layer leading to an increase in the trapped Au concentration at the EOR damage, with a corresponding decrease from the near-surface region (shown in Fig. 3 (e)). The concentration of Au trapped in the EOR damage layer has been found to increase further for the subsequent 20 minute annealing step at 950°C (Fig. 3 (f)). The observed enhancement in the gettering efficiency of EOR damage layer for annealing at temperatures higher than 750°C is really striking.

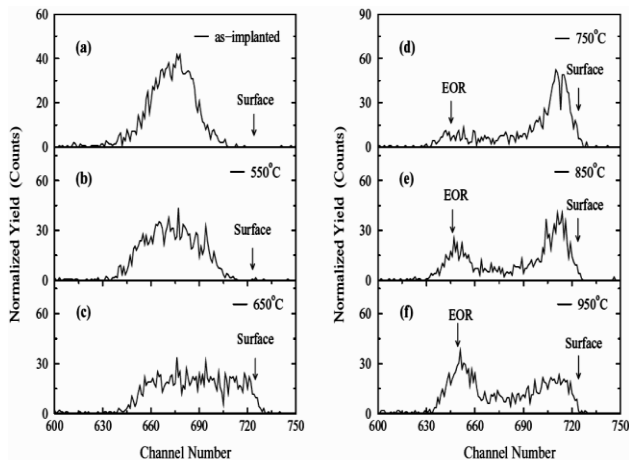


Fig. 3. RBS spectra showing the Au profiles in Si implanted with Au to a dose of 2.2×10^{15} ions cm⁻² and isochronally annealed for 20 minutes at temperatures varying from 550 - 950°C followed by rapid quenching in liquid N₂.

In Fig. 4 we show the variation of concentration of Au trapped at the EOR damage layer with annealing temperature. It can be seen that the trapped Au concentration increases linearly with increase in annealing temperature beyond 750°C. The amount of Au trapped at EOR damage layer has been estimated to be $\sim 9 \times 10^{14}$ atoms cm⁻², which is very high (about 41% of the Au dose). It clearly indicates that upon isochronal annealing

the EOR defects are evolving into stronger gettering centers for diffusing Au atoms, with increase in annealing temperature to 950°C. Since the gettering efficiency of any defect for diffusing Au atoms is strongly dependent on its trapping efficiency for Si interstitials, it can be inferred that the EOR defects are transforming into more stable defect structures, which efficiently trap Si interstitials and hence efficiently getter Au atoms.

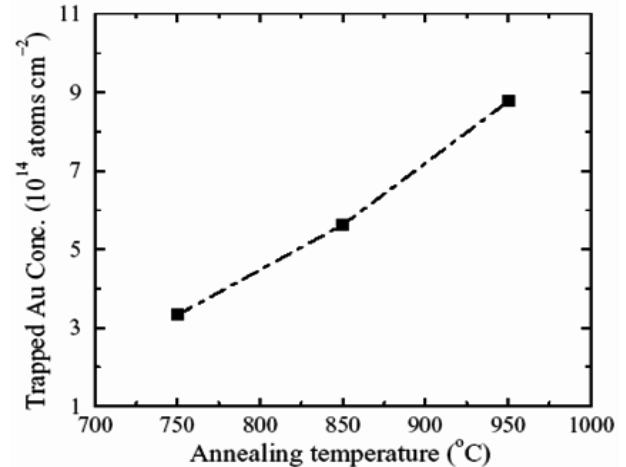


Fig. 4. Dependence of the concentration of Au trapped at the EOR damage layer on annealing temperature.

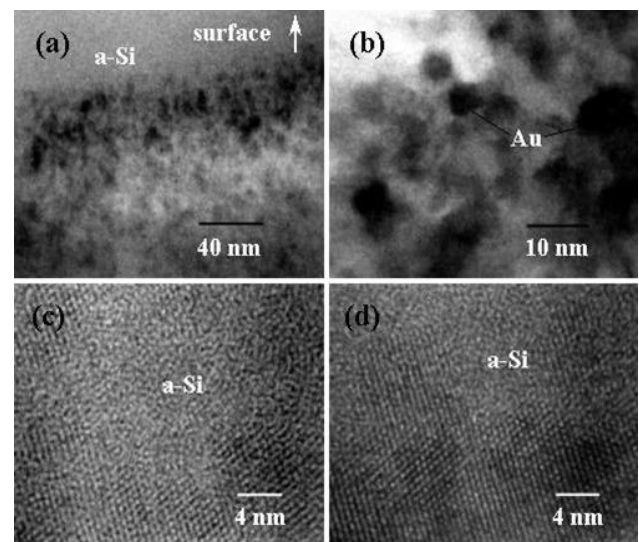


Fig. 5. Bright field XTEM images of Si(111) substrate implanted with 1.5 MeV Au²⁺ ions to a dose of 2.2×10^{15} ions cm⁻² at room temperature showing (a) damage layer around the projected range of Au ions, (b) Higher magnification image showing Au-rich regions embedded in amorphous Si layer, (c-d) High resolution TEM images of the amorphous-crystalline (a/c)-interface around the EOR of Au implant.

Fig. 5 (a-b) shows the bright field XTEM images showing the microstructure of Si(111) implanted with 1.5 MeV Au ions to a dose of 2.2×10^{15} ions cm⁻². The presence of a thick amorphous Si (a-Si) layer extending from the projected range of Au up to the surface was observed. The damage layer around the projected range was found to contain nanosized Au-rich precipitates and defects. The HRTEM images of the amorphous-crystalline (a/c) interface in the EOR damage layer are

shown in **Figs 5 (c-d)**, which clearly show the interface of nanoscale amorphous regions with crystalline Si layer below. The evolution of the microstructure of the Au implanted Si(111) sample upon thermal annealing is studied by XTEM. The bright field XTEM images showing the microstructure of Si(111) implanted with 1.5 MeV Au ions to a dose of 2.2×10^{15} ions cm^{-2} annealed at 850°C for 1 h are shown in **Figs 6 (a-b)**. Annealing at 850°C has been found to result in solid phase epitaxial recrystallization of the surface amorphous Si layer and formation of a highly defected near-surface region. The presence of dislocations with few of them reaching up to the surface can be clearly seen in this region (**Fig. 6 (a)**). Few Au-rich precipitates were also observed in the strain fields of these dislocations. The EOR damage layer was found to consist of dislocation loops, as can be seen from **Fig. 6 (b)**. HRTEM images of the precipitates trapped around dislocations are shown in **Figs 6 (c-d)**. The Moire fringes seen in **Fig. 6 (c)** confirm the presence of Au-Si precipitates. **Fig. 6 (d)** shows the HRTEM image of a precipitate trapped around a dislocation which shows the presence of lattice fringes corresponding to Au nanoparticle in face centered cubic phase embedded in crystalline Si.

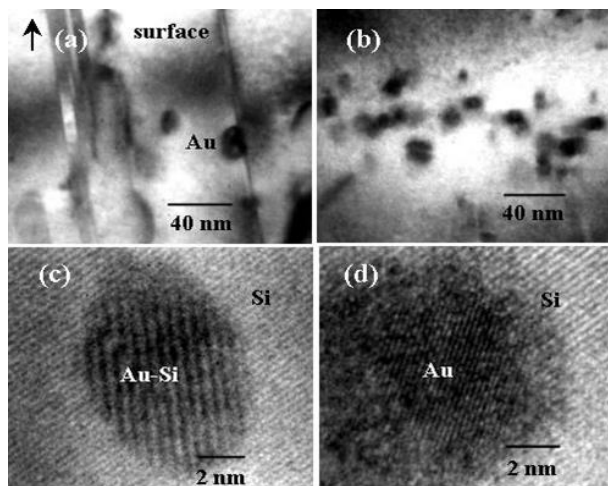


Fig. 6. Bright field XTEM images of Si(111) substrate implanted with 1.5 MeV Au^{2+} ions to a dose of 2.2×10^{15} cm^{-2} and annealed at 850°C for 1 h showing (a) dislocations mediating out-diffusion of Au in Si, (b) EOR dislocation loops containing nanosized Au precipitates, High resolution TEM images showing (c) Moire fringes associated with nanosized Au_5Si_2 phase and (d) lattice fringes of Au nanoparticle trapped at dislocations in Si.

The observed enhanced Au gettering behavior of EOR dislocation loops in Si can be understood as follows. 1.5 MeV Au^{2+} implantation to a fluence of 2.2×10^{15} ions cm^{-2} leads to the formation of continuous surface amorphous layer in Si(111) [15]. Annealing in the temperature range of 550-650°C is known to mark the onset of solid phase epitaxial recrystallization of the amorphous Si layer. Recrystallization starts from the original amorphous-to-crystalline (a/c) interface. Since the solid solubility of Au in c-Si is orders of magnitude lower than in a-Si, recrystallization of the amorphous layer leads to rejection of Au atoms ahead of the

recrystallizing interface. During annealing at 650°C, Au atoms get uniformly distributed in the a-Si layer extending up to the surface. At 650°C the diffusivity of Au in a-Si is so high that Au outruns the interface, leading to a fairly uniform flat-topped profile. Subsequent annealing at 750°C leads to solid phase epitaxial recrystallization of a-Si layer. This results in the rejection of Au into the defected polycrystalline layer in the near-surface region. Dislocations formed in the near-surface region mediate rapid 'pipe diffusion' of Au atoms towards surface. This results in the observed enhanced out-diffusion of Au atoms in Si. The Au atoms get trapped in the strain fields of dislocations and cluster forming Au nanoparticles, which can be clearly seen from the HRTEM results (as shown in **Fig. 6 (d)**). However, annealing at 750°C leads to the clustering of Si interstitials left below the a/c-interface resulting in the formation of rod-like {311} defects and dislocation loops at EOR [6-7]. Prolonged annealing at 750°C leads to a reduction in the number of Si interstitials bound to {311} defects leading to their dissolution, while the emitted Si interstitials are absorbed by dislocation loops which grow in size and number density [16]. Annealing at temperatures $\geq 850^\circ\text{C}$ leads to the dissolution of {311} defects, which emit Si interstitials feeding the growth of existing dislocation loops at EOR [7]. In addition, the emitted Si interstitials cluster forming new dislocation loops at EOR. This results in an increased number density of EOR dislocation loops [7]. The newly formed and the growing dislocation loops at EOR act as efficient trapping sites for Si interstitials and hence efficiently trap diffusing Au atoms, making them immobile Au_s atoms. This results in an increase in trapped Au concentration at EOR. Our results, showing an increase in Au gettering efficiency of EOR damage layer, are in excellent agreement with this. The observed enhanced Au gettering efficiency of EOR defects can be ascribed to the formation of dislocation loops with increased number density at EOR which act as highly stable and efficient gettering centers for Si interstitials and hence diffusing Au atoms in Si.

Conclusions

In summary, we have investigated the gettering behavior of EOR defects for Au atoms in Si(111). For annealing at 750°C pronounced out-diffusion of the implanted Au atoms along with gettering of Au at EOR damage layer has been observed. Beyond 750°C the gettering efficiency of the EOR damage layer has been found to increase with increase in annealing temperature, reaching 41% at 950°C. The enhanced gettering efficiency of EOR damage layer clearly indicates that upon isochronal annealing at 950°C the EOR defects are evolving into stronger gettering centers for Au atoms in Si. This is ascribed to the increased formation of dislocation loops which on high temperature annealing grow and evolve into more stable and efficient trapping centers for diffusing Au atoms in Si. The observed enhanced gettering efficiency of EOR defects is very promising for gettering applications in Si devices.

Acknowledgements

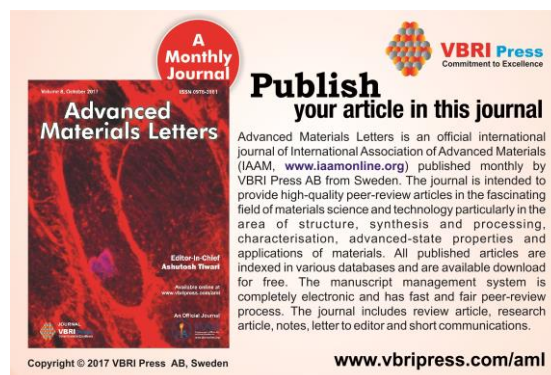
The author would like to thank the operators of Ion Beam Laboratory, Institute of Physics, Bhubaneswar for their support and Prof. D. P. Mahapatra for useful discussions.

Author contributions

Conceived the plan: SM; Performed the experiments: SM; Data analysis: SM; Wrote the paper: SM (SM is the initial of author). Author has no competing financial interests.

References

- 1 Eaglesham, D. J.; Stolk, P. A.; Gossmann, H. J. and Poate, J. M. *Appl. Phys. Lett.* **1994**, *65*, 2305.
DOI: <http://dx.doi.org/10.1063/1.112725>
- 2 Rafferty, C. S.; Gilmer, G. H.; Jaraiz, M.; Eaglesham, D. and Gossmann, H. J. *Appl. Phys. Lett.* **1996**, *68*, 2395.
DOI: <http://dx.doi.org/10.1063/1.116145>
- 3 Chao, H. S.; Griffin, P. B.; Plummer, J. D. and Rafferty, C. S. *Appl. Phys. Lett.* **1996**, *69*, 2113.
DOI: <http://dx.doi.org/10.1063/1.116897>
- 4 Liu, J.; Krishnamoorthy, V.; Gossmann, H. J.; Rubin, L.; Law, M. E. and Jones, K. S. *J. Appl. Phys.* **1997**, *81*, 1656.
DOI: <http://dx.doi.org/10.1063/1.364022>
- 5 Bonafos, C.; Martinez, A.; Faye, M. M.; Bergaud, C.; Mathiot, D. and Claverie, A. *Nucl. Instrum. Meth. B* **1995**, *106*, 222.
DOI: [http://dx.doi.org/10.1016/0168-583X\(95\)00707-5](http://dx.doi.org/10.1016/0168-583X(95)00707-5)
- 6 Jones, K. S.; Liu, J.; Zhang, L.; Krishnamoorthy, V. and DeHoff, R. T. *Nucl. Instrum. Meth. B* **1995**, *106*, 227.
DOI: [http://dx.doi.org/10.1016/0168-583X\(95\)00708-3](http://dx.doi.org/10.1016/0168-583X(95)00708-3)
- 7 Li, J. and Jones, K. S. *Appl. Phys. Lett.* **1998**, *73*, 3748.
DOI: <http://dx.doi.org/10.1063/1.122882>
- 8 Liefing, J. R.; Schretelkamp, R. J.; Vanhellefont, J.; Vandervorst, W.; Maex, K.; Custer, J. S. and Saris, F. W. *Appl. Phys. Lett.* **1993**, *63*, 1134.
DOI: <http://doi.org/10.1063/1.109803>
- 9 Stolk, P. A.; Gossmann, H. J.; Eaglesham, D. J.; Jacobson, D. C.; Rafferty, C. J.; Gilmer, G. H.; Jaraiz, M.; Poate, J. M.; Luftman, H. S. and Haynes, T. E. *J. Appl. Phys.* **1997**, *81*, 6031.
DOI: <http://doi.org/10.1063/1.364452>
- 10 Park, H.; Robinson, H.; Jones, K. S. and Law, M. E. *Appl. Phys. Lett.* **1996**, *65*, 436.
DOI: <http://doi.org/10.1063/1.112325>
- 11 Frank, F. C. and Turnbull, D. *Phys. Rev.* **1956**, *104*, 617.
DOI: <https://doi.org/10.1103/PhysRev.104.617>
- 12 Gosele, U.; Frank W. and Seeger, A. *Appl. Phys.* **1980**, *23*, 361.
DOI: [10.1007/BF00903217](https://doi.org/10.1007/BF00903217)
- 13 Mahapatra, S.; Joseph, B.; Satpati, B.; Mahapatra, D. P. *Appl. Phys. A* **2006**, *82*, 297.
DOI: [10.1007/s00339-005-3297-y](https://doi.org/10.1007/s00339-005-3297-y)
- 14 Mahapatra, S.; Mahapatra, D. P. *Nucl. Instrum. Meth. B* **2004**, *222*, 249.
DOI: <http://dx.doi.org/10.1016/j.nimb.2004.01.215>
- 15 Kamli, J.; Satpati, B.; Goswami, D. K.; Rundhe, M.; Dev, B. N.; Satyam, P. V. *Nucl. Instrum. Meth. B* **2003**, *207*, 291.
DOI: [http://dx.doi.org/10.1016/S0168-583X\(03\)00459-2](http://dx.doi.org/10.1016/S0168-583X(03)00459-2)
- 16 Robertson, L. S.; Jones, K. S.; Rubin, L. M.; Jackson, J. J. *Appl. Phys.* **2000**, *87*, 2910.
DOI: <http://doi.org/10.1063/1.372276>



A Monthly Journal

Publish your article in this journal

Advanced Materials Letters is an official international journal of International Association of Advanced Materials (IAAM, www.iaamonline.org) published monthly by VBRI Press AB from Sweden. The journal is intended to provide high-quality peer-review articles in the fascinating field of materials science and technology particularly in the area of structure, synthesis and processing, characterisation, advanced-state properties and applications of materials. All published articles are indexed in various databases and are available download for free. The manuscript management system is completely electronic and has fast and fair peer-review process. The journal includes review article, research article, notes, letter to editor and short communications.

Copyright © 2017 VBRI Press AB, Sweden www.vbripress.com/aml